Fuel 220 (2018) 233–239

Contents lists available at ScienceDirect

Fuel

journal homepage: www.elsevier.com/locate/fuel

Full Length Article

A new prediction method for the viscosity of the molten coal slag. Part 2: The viscosity model of crystalline slag

Jie Zhou[a,b], Zhongjie Shen[a,b], Qinfeng Liang[a,b,c], Jianliang Xu[a,b], Haifeng Liu[a,b,*]

[a] Key Laboratory of Coal Gasification and Energy Chemical Engineering of Ministry of Education, East China University of Science and Technology, P.O. Box 272, Shanghai 200237, PR China

[b] Shanghai Engineering Research Center of Coal Gasification, East China University of Science and Technology, P.O. Box 272, Shanghai 200237, PR China

[c] State Key Laboratory of Coal Conversion, Institute of Coal Chemistry, Chinese Academy of Sciences, Taiyuan, PR China

ARTICLE INFO

Keywords:
Coal
Crystalline slag
Crystal morphology
Viscosity model

ABSTRACT

The complex chemical composition of coal slag separated out different types and shapes of crystals during the cooling process. The morphology of the crystal in the molten slag influenced the viscosity of the coal slag. The aim of this paper was to obtain the viscosity model of crystalline slag using a new calculation method. The model of the suspension viscosity obtained by the previous study was used to predict the viscosity of molten slag. The correction factor (β) was introduced in the model of the suspension viscosity. The solid phase volume fraction (φ) in the molten slag was calculated by FactSage. The liquid phase viscosity (η_0) was fitted by the viscosities of molten slag in high temperature section. Ten kinds of crystalline slags were applied in this study to prove the accuracy of the modified viscosity model. The viscosity of molten slag predicted by the model (CSM) agreed with experiment data.

1. Introduction

Entrained flow gasification technology is a type of clean coal conversion technology, which plays an important role in reducing carbon dioxide emissions and improving energy efficiency. It allows for various combinations of electricity, liquid fuels, hydrogen, chemicals and heat with the characters of high efficiency and fuel flexibility [1]. Entrained flow gasifier usually operates at high temperature (above the ash flow temperature) to ensure a suitable slagging condition for the stable operation [2,3]. The viscosity of molten slag is the key factor in determining whether the slagging condition is smooth and stable. The viscosity of molten slag exhibited a rapid increase because of the increase of crystals in the molten slag when temperature was lowered below a certain temperature which was referred as the temperature of critical viscosity (T_{cv}) [4,5].

Many factors affect the viscosity of molten slag, including composition, cooling rate, residence time and so on. And these factors influence the viscosity of molten slag by changing the volume fraction of crystal phase in the molten slag. A number of scholars have studied the factors that affect the crystallization of slag. Fredericci et al. [6] considered the crystallization mechanism of an unaltered blast-furnace slag composition. They suggested that most crystallization was on surface and this suggestion was confirmed by the study of nucleation kinetics. Xuan et al. [7–10] studied the influences of CaO, Fe_2O_3, SiO_2/Al_2O_3 on crystallization characteristics of synthetic coal slags. With the increase of CaO, crystallization of the slag became significant, especially in those with a calcium range between 15% and 35%. The crystallization temperature increased but only slightly. With a higher ratio of Fe_2O_3, more crystallization heat was released and the crystallization shifted to a higher temperature, potentially leading to a higher T_{cv} in viscosity. The kinetics under isothermal 1100 °C showed that the growth rate of crystals increased with the addition of iron oxide. As the S/A ratio increased in the range from 1.5 to 3.5, energy barrier was significantly lowered which increased the crystallization ratio. Shen et al. [11] studied the effect of cooling process on the generation and growth of crystals in coal slag. The variation of the cooling process obviously affected the crystallization behavior of molten slag. Low cooling rate benefited the generation of the crystals and long residence time below the initial crystallization temperature promoted the generation and growth of crystal. Louhich et al. [12] reproduced the experimental T dependence of the crystallization temperature with numerical calculations based on standard models for the nucleation and growth of hard-sphere crystals, classical nucleation theory and the Johnson-Mehl-Avrami-Kolmogorov theory. These results suggested that deep analogies existed between hard-sphere colloidal crystals and pluronics micellar crystals, in spite of the difference in particle softness. Studies about

* Corresponding author at: Key Laboratory of Coal Gasification and Energy Chemical Engineering of Ministry of Education, East China University of Science and Technology, P.O. Box 272, Shanghai 200237, PR China.
E-mail address: hfliu@ecust.edu.cn (H. Liu).

https://doi.org/10.1016/j.fuel.2018.01.056
Received 9 September 2017; Received in revised form 30 November 2017; Accepted 16 January 2018

glassy slag are relatively rich in the glass industry. Karamanov et al. [13] summarized results of the crystallization of iron-rich glasses. The results indicated that magnetite and pyroxene were the main crystal phases and that the kinetics of pyroxene formation could be explained as growth on a fixed number of magnetite nuclei. Pacurariu et al. [14] studied non-isothermal crystallization kinetics of some glass-ceramics with pyroxene structure. Many other scholars [15–19] have also studied the effect of other factors on the slag crystallization process including residual carbon, trace elements and so on.

About the viscosity of molten slag, Kondratiev et al. [20], Ilyushechkin et al. [21] and Zhang et al. [22] studied the characters of flowability and T_{cv} of coal ash slag. Kong et al. [23–25] proposed the internal and external factors influencing the slag viscosity at high temperature, including CaO content, residual carbon and cooling rate. It was found that the viscosities of both the glassy and the crystalline slag were declining when the cooling rate increased. However, when the temperature was lower than the flow temperature, the impact of the cooling rate on crystal slag was more obvious. At the same time, T_{cv} also decreased with increasing cooling rate. Residual carbon in the slag was the internal factor affecting the slag viscosity. With the content of residual carbon increasing, the slag viscosity also increased. When the content of residual carbon was more than 5%, a significant impact on the slag viscosity appeared. They also studied the effect of CaO content on the viscosity curve. When the CaO content increased, the slag viscosity increased, which exhibited the same properties as the viscosity of crystal slag versus S/A ratio. Other documents also mentioned the influence of silicon, aluminum and other trace elements on the slag viscosity. Zhang et al. [26] found that the viscosity of CaO-SiO_2-Al_2O_3-CaF_2 system increased monotonously with gradually increasing substitution content of Al_2O_3 for SiO_2. Feng et al. [27] produced that the viscosity of slag decreased with the increase of TiO_2 content. Wang et al. [28] found that the viscosity of liquid slag decreased with the addition of V_2O_5 increasing at high temperature. Ilyushechkin et al. [29] studied the viscosity of high-iron slags from Australian coal. Folkedahl et al. [30] considered the effect of atmosphere on the viscosity of selected bituminous and low-rank coal ash slags. Under the air atmosphere, the slag viscosity was related to the mole ratio of basic to acidic oxides. However, the changes in viscosity observed in using hydrogen instead of air atmosphere appeared to be related to the amount of iron which was originally in the slag.

Kondratiev et al. [31], Hosseini et al. [32], and Ramacciotti et al. [33] have proposed models to predict the slag viscosity. These models were based on the method of simplifying the synthesis of oxides, so there were great limitations in the accuracy of prediction. Browing et al. [34] proposed a classical prediction method for the viscosity of molten slag which exhibited Newtonian fluid properties. Fulcher et al. [35] proposed the viscosity prediction model based on temperature correction factor by using Arrhenius equation:

$$\log\eta = A + \frac{B}{T-T_0}. \tag{1}$$

where A is a constant, B is the activation energy, and T_0 is the temperature correction factor.

Urbain et al. [36] established the semi-empirical model to predict the viscosity of Al_2O_3-CaO-FeO-SiO_2 system according to Weymann-Frenkel equation [37], which was the most widely used in recent years.

$$\eta = aTe^{1000b/T}, \tag{2}$$

and

$$\ln(a) = -0.2963b - 11.6725. \tag{3}$$

In the equation above, T is the slag temperature, the unit is K. a and b are the empirical constants, b is related to the slag composition, as a function of the slag system components. Many other researchers, such as Kalmanovitch and Frank [38], Kondratiev and Jak [39] and Hurst et al. [40] had also modified the Urbain model.

Table 1
Chemical composition of coals in the experiment.

Composition/wt%	SiO_2	CaO	Al_2O_3	Fe_2O_3	MgO	Na_2O	TiO_2
SF	37.65	26.16	19.69	11.89	0.96	2.62	1.03
YL	27.20	28.12	25.44	16.65	1.07	0.77	0.48
JJT	32.19	25.91	19.85	16.12	3.12	2.31	0.49
YH	26.66	22.27	20.31	24.98	3.01	2.37	0.41
BD	45.23	36.09	9.51	4.55	1.40	1.10	2.11
NM	48.85	16.22	13.28	15.88	3.42	1.64	0.71
TX	50.26	30.42	1.72	11.82	0.56	2.17	3.05
XJW	50.10	30.67	1.53	11.95	0.56	2.16	3.04
BS	39.31	23.89	9.65	21.20	3.23	1.29	1.45
ZX	55.23	21.97	0.20	19.24	0.55	2.04	0.78

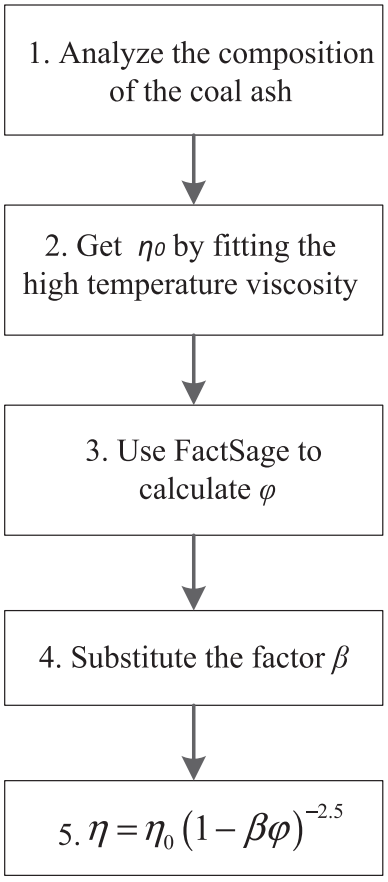

Fig. 1. Schematic diagram of the calculation method.

Reid [41] suggested that the viscosity of the slag at a given temperature can be expressed as an expression of SiO_2 content. Watt et al. [42] studied the viscosity of homogeneous liquid slag in relation to slag composition. The equation was given by

$$\log\eta = \frac{10^7 m}{(T-150)^2} + c, \tag{4}$$

where η is in poise, and T is in °C. Here

$$m = 0.00835SiO_2 + 0.00601Al_2O_3 - 0.109, \tag{5}$$

and

$$c = 0.0415SiO_2 + 0.0192Al_2O_3 + 0.0276(equiv.\ Fe_2O_3) + 0.0160CaO - 3.92, \tag{6}$$

and slag components are expressed on weight percentages.

It can be seen from the literatures that bulk of irregular crystals generated in the crystalline slag during the crystallization process which improved the difficulty in predicting the viscosity of the

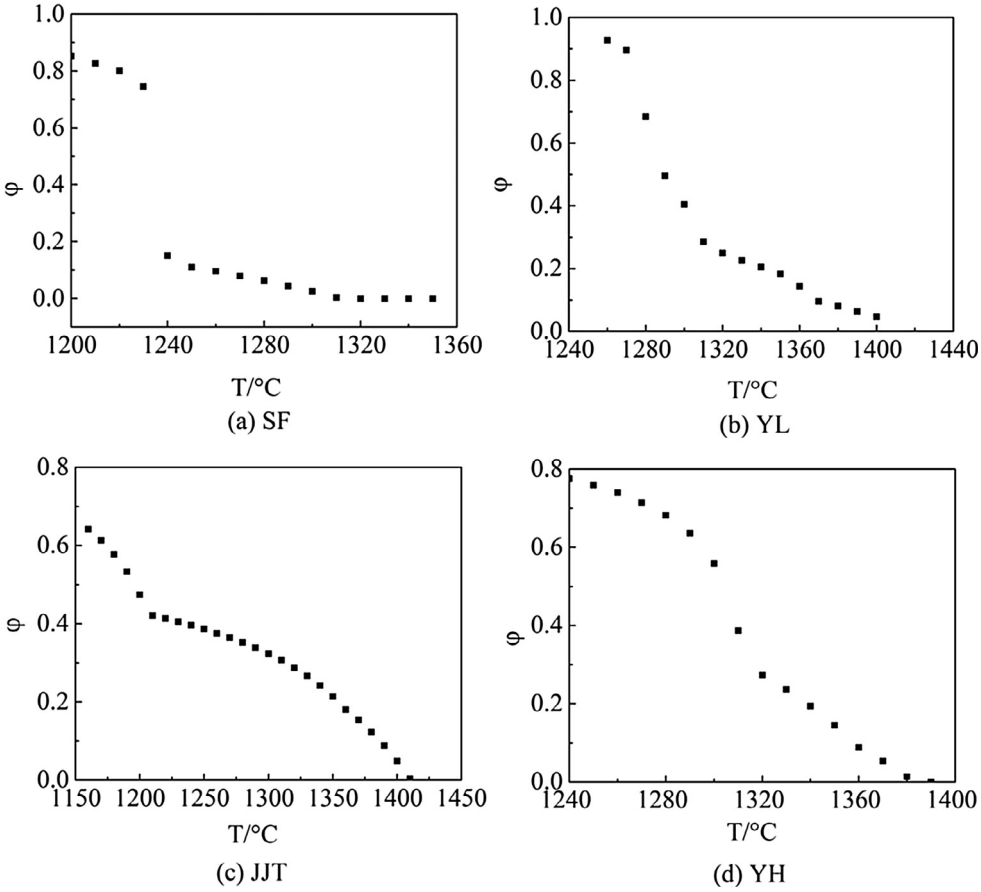

Fig. 2. Variation of solid phase volume fraction of different coal slags with temperature.

crystalline slag, especially the viscosity near T_{cv}. Therefore, a new model (CSM) for calculating the viscosity of crystalline slag was obtained by using the relationship between the suspension viscosity and the solid phase volume fraction in this paper. Correction parameter (β) was introduced to modify the equation. The liquid phase viscosity (η_0) was fitted by the viscosity of molten slag in high temperature section. Ten kinds of crystalline coal samples were used to verify the accuracy of the model.

2. Experiment

2.1. Experiment sample

Ten kinds of crystalline coal samples were used to prepare the coal ash in the N17/HR-K muffle furnace (Nabertherm Company, Lilienthal, Germany), according to the Chinese standard GB/T1574-2007. In the experiment of coal ash preparation, the temperature first rose from room temperature to 500 °C within 30 min and then was held for another 30 min to remove the water of crystallization. Then the temperature was heated to 815 °C within 30 min and held for about 120 min for the complete reaction of coal and air. The aim of the process was to obtain coal ash samples with inorganic minerals. The coal ash sample was analyzed by Advant'X Intellipower 3600 X-ray fluorescence (Thermo Fisher Scientific, America) [11]. The ash compositions of the ten coal samples are shown in Table 1.

2.2. Experiment equipment and method

2.2.1. High temperature viscosity measurement

Viscosity measurement instrument is RV DVIII type high temperature rotary viscometer produced by Theta in America [17]. It mainly consists of the following parts: Brookfield DVIII rheometer, high temperature heating furnace, gas circulation system, water cooling system, temperature control system and data acquisition system. The DilaSoft32 software on the computer controls and records the temperature data of the furnace. The high temperature heating furnace of the viscometer was heated by the silicon aluminum rod, whose maximum temperature could reach to 1700 °C. The height and diameter of the cylindrical corundum crucible were 120 and 30 mm. The height and diameter of the spindle were 16 and 12 mm. Before the measurement, the rheometer should be calibrated through the standard silicone oil, and the measurement error was controlled within 1%. During the viscosity test, approximately 45 g of coal ash was placed in a ceramic corundum crucible and fixed by a corundum bracket of the high temperature furnace. The entire heating zone and reaction zone were sealed by metal flanges and vacuum evacuated for 5 min using a vacuum pump. The gas CO/CO_2 (molar ratio 60/40) was then fed from the bottom of the furnace and the gas flow rate was 100 ml/min to create a reducing atmosphere. The gas was removed from the top of the furnace in order that the sample was in a reducing atmosphere. The ash sample was heated from room temperature to a temperature higher than the ash melting temperature of 200 °C at a rate of 5 °C/min in the heating furnace. The entire rotor was then slowly put down below the slag level and the temperature should be kept at a constant value for 30 min to measure the slag viscosity smoothly.

3. Results and discussion

3.1. Viscosity model

It can be seen from the previous studies that the morphology of the crystals in the molten slag was mainly acicular and occupied a large

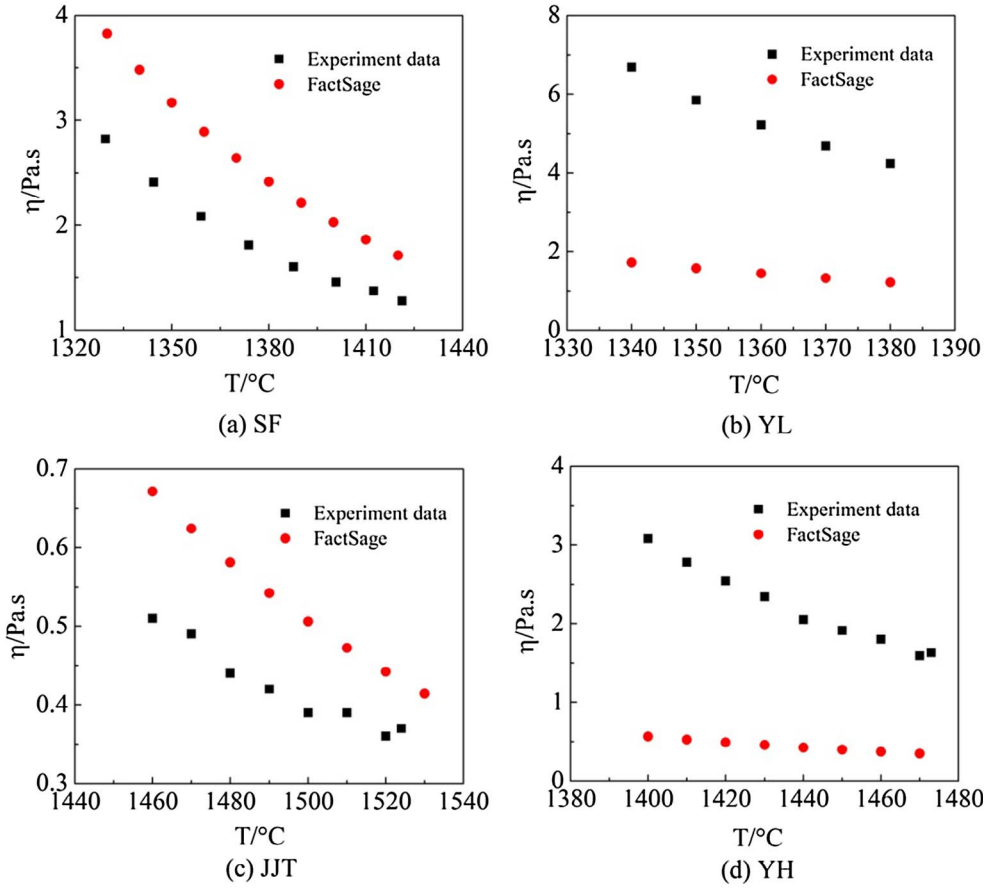

Fig. 3. Variation of viscosity with high temperature range of different coal slags.

Table 2
Viscosity equations of high temperature section of different coals.

Sample	η_{0c}	η_{0e}
SF	$4.261 \times 10^{8}e^{-0.0142T}$	$3.831 \times 10^{5}e^{-0.0089T}$
YL	$4.302 \times 10^{4}e^{-0.0076T}$	$3.436 \times 10^{7}e^{-0.0115T}$
JJT	$7.115 \times 10^{3}e^{-0.0064T}$	$1.556 \times 10^{3}e^{-0.0055T}$
YH	$1.192 \times 10^{3}e^{-0.0059T}$	$1.068 \times 10^{6}e^{-0.0091T}$

volume fraction during the slag crystallization process. A number of crystals had great influence on the viscosity of molten slag during crystallization process. Through the previous study, a modified model of the suspension viscosity respecting to the solid phase volume fraction was obtained as follows:

$$\eta = \eta_0(1-\beta\varphi)^{-2.5}, \tag{7}$$

and

$$\beta = 0.9672Ce^{-0.0022d}e^{0.0126(\theta-1)}, \tag{8}$$

where η_0 was Newtonian viscosity of the suspending liquid, β was the correction factor, d was the particle size, and θ was the particle aspect ratio. C was a constant related to the shape of the particle. When the particles were spherical, C was 1. When the particles were non-spherical, C was 1.235. Therefore, Eq. (7) was used to calculate the slag viscosity. The schematic diagram of the calculation method is shown in Fig. 1.

The calculation steps are as follows: 1. X-ray Fluorescence (XRF) was used to analyze the different coal ashes, including the main components of the oxide composition and content. 2. High temperature rotary viscometer and FactSage were used to calculate the slag viscosities at different temperatures. And the viscosity of the high temperature section obtained by the two methods were fitted as the liquid phase viscosity (η_0) of the molten slag. The liquid phase viscosity obtained by the experiment data was denoted as η_{0e}, and the liquid phase viscosity calculated by FactSage was denoted as η_{0c}. 3. FactSage was used to calculate the solid phase volume fraction (φ) under the composition mentioned above, where the volume fraction was instead of the mass fraction. 4. According to the conclusion given by Shen et al. [11] on the changes of crystal shape and aspect ratio during the crystallization process. It can be concluded that the average crystal size was 50 μm, the average crystal aspect ratio was 10 and the constant C took 1.235. The Eq. (8) was used to obtain the correction factor β with the value of 1.19. 5. The corresponding temperature and the solid phase volume fraction were substituted into Eq. (7) to calculate the viscosity at different temperatures and finally get the viscosity-temperature curves.

3.2. Model verification

3.2.1. Changes of the solid phase volume fraction with the temperature

In this paper, the viscosities of ten typical crystalline coal slags were calculated by Eq. (7). The ash compositions of the ten coal samples are shown in Table 1.

Fig. 2 shows the changes of solid phase volume fraction with temperature of different coal slags (SF, YL, JJT and YH). It can be seen from the Fig. 2 that with the decrease of temperature, the solid phase volume fraction in the molten slag increased, and when the temperature reached a certain temperature, the solid phase volume fraction increased rapidly. This phenomenon indicated that the increment of crystal was violent at this time. For SF, YL, JJT and YH, the temperatures were about 1230 °C, 1280 °C, 1310 °C and 1315 °C respectively.

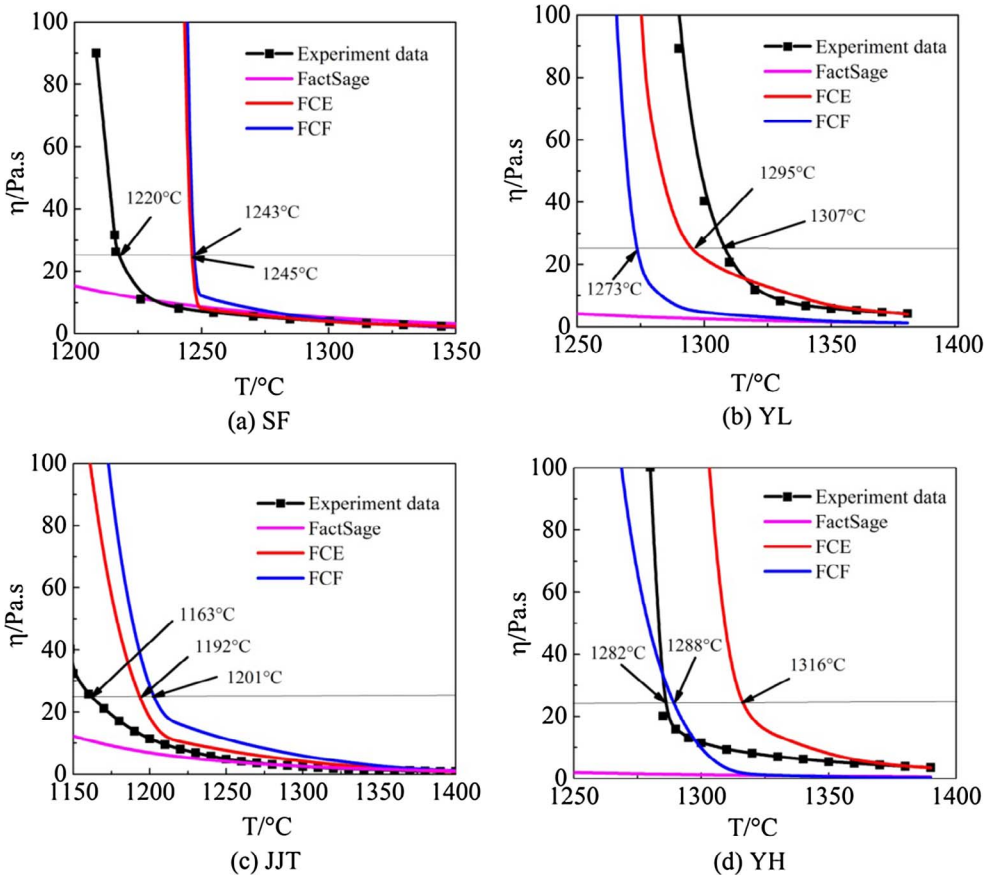

Fig. 4. Viscosity-temperature curves of different coal samples.

Table 3
Comparison of characteristic temperature of different coals.

Sample	T_{25}/°C	$\triangle T_{25\text{-}c}$/°C	$\triangle T_{25\text{-}e}$/°C	T_{cv}/°C	$\triangle T_{cv\text{-}c}$/°C	$\triangle T_{cv\text{-}e}$/°C
SF	1220	25	23	1228	15	13
YL	1307	−34	−12	1326	−35	−15
JJT	1163	38	29	1158	50	46
YH	1282	34	6	1285	34	19
BD	1372	5	71	1380	10	66
NM	1286	−14	−60	1290	5	10
TX	1375	60	35	1395	20	10
XJW	1455	−29	−31	1470	−33	−35
BS	1295	15	16	1298	16	17
ZX	1364	41	16	1380	35	30
Average error		14.1	9.3		11.7	16.7

The abrupt change point of the solid phase volume fraction had great influence on T_{cv}. When the temperature was further decreased, the increase rate of the solid phase volume fraction decreased, indicating that the growth of crystal in the slag was basically complete. Shen et al. [11] found that the number of crystals increased with the increase of the residence time. The influence of residence time was not considered by FactSage. Therefore, the solid phase volume fraction calculated by FactSage had a little difference with the experimental value at the same temperature.

3.2.2. The viscosity of molten slags at high temperature

The changes of liquid phase viscosity with temperature in different high temperature range of molten slag were shown in Fig. 3. In Fig. 3, slag viscosity increased with the temperature decreasing, but the rise of the viscosity was small. This phenomenon indicated that no crystal was formed in slag and the slag was still in the molten state. Therefore, it was reasonable to use the viscosity data of the high temperature range to fit the equation of the liquid phase viscosity. The fitting equations obtained from different coal samples were shown in Table 2. Among them, η_{0c} was the viscosity of the slag in the high temperature section calculated by FactSage, η_{0e} was the viscosity of the slag in the high temperature section obtained by the experimental data. And T was the slag temperature in units of K. Although the viscosity of slag in the high temperature section obtained by the two methods had a certain difference, the difference of absolute viscosity was small. The viscosity temperature curves of different coals were obtained by the liquid phase viscosity in the high temperature section of two methods.

3.2.3. Viscosity prediction

The comparison of the viscosity predicted by model with the experiment data is shown in Fig. 4. The black curve represented the changes of viscosity measured by experiment, and the pink curve represented the changes of viscosity calculated by FactSage. The red curve (FCE) showed the changes of viscosity whose liquid phase viscosity was obtained from the experiment data, and the blue curve (FCF) indicated that the changes of viscosity whose liquid phase viscosity was obtained by the FactSage. It can be seen from the Fig. 4 that the viscosity calculated by the model was consistent with the trend of viscosity measured by the actual measurement and the difference in the value was small. In the actual project, the requirement of the slag viscosity was below 25 Pa.s. So 25 Pa.s was chosen for the critical point for analysis in this paper. The comparison of the characteristic temperatures of the different coals samples is shown in Table 3. When the viscosity was 25 Pa.s, the temperature difference between the actual value and the model whose liquid phase viscosity was calculated from FactSage ($\triangle T_{25\text{-}c}$) were 25, −34, 16 and 34 °C respectively. The average error of $\triangle T_{25\text{-}c}$ was 14.1 °C. The temperatures difference between the actual value and the model whose liquid phase viscosity was calculated

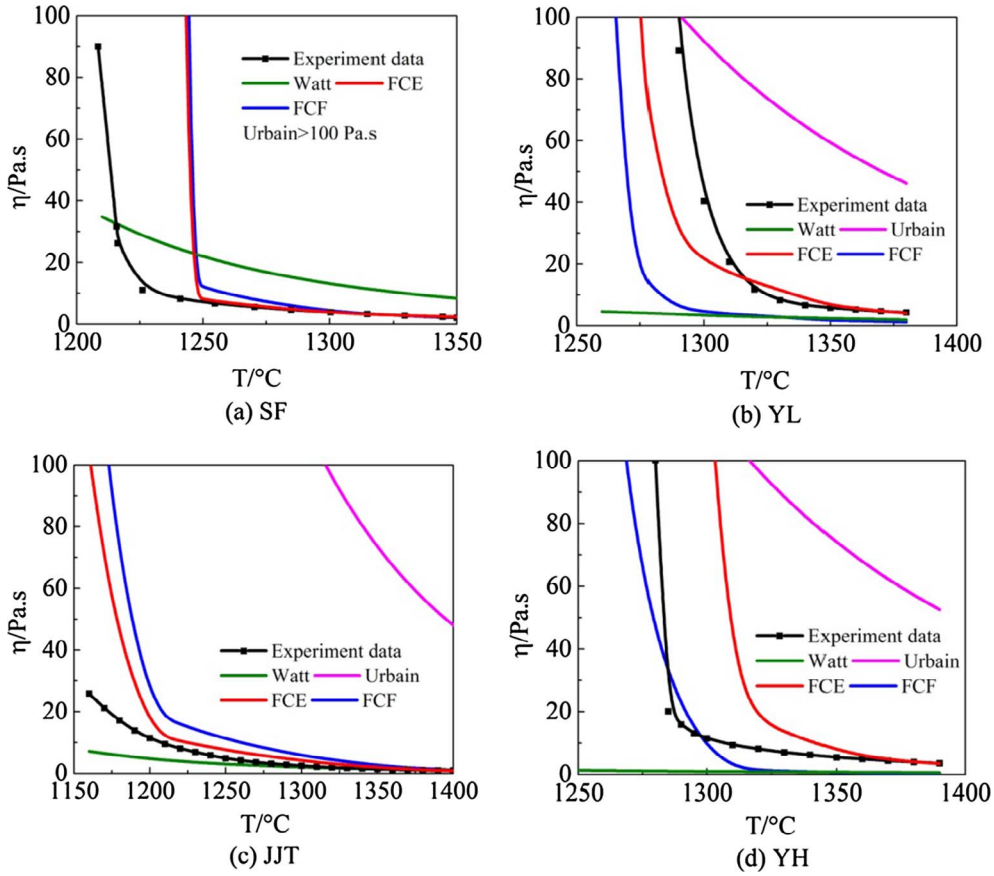

Fig. 5. Comparison of the measured viscosities predicted by the proposed methods for different coal samples.

from experiment data ($\triangle T_{25\text{-}e}$) were 23, −12, 14 and 6 °C respectively. The average error of $\triangle T_{25\text{-}e}$ was 9.3 °C. For the critical viscosity point (T_{cv}), the temperature difference between the experimental data and the model whose liquid phase viscosity was calculated from the FactSage ($\triangle T_{cv\text{-}c}$) were 15, −35, 15 and 34 °C respectively. The average error of $\triangle T_{cv\text{-}c}$ was 11.7 °C. The temperature difference between the actual value and the model whose liquid phase viscosity was obtained by the experimental data ($\triangle T_{cv\text{-}e}$) were 13, −15, 13 and 19 °C respectively. The average error of $\triangle T_{cv\text{-}e}$ was 16.1 °C. In conclusion, the average error of characteristic temperatures of different coal samples obtained by the model was below 20 °C. The results illustrated that the model had advantages in predicting the viscosity of crystalline slags. However, it can also be seen from the Fig. 4 that the viscosity value calculated by FactSage differed from the viscosity value measured by experiment. The difference was mainly due to the fact that the calculation of FactSage was based on the phase equilibrium principle. This principle was different from the actual situation. Thus little difference in viscosity was existed.

3.3. Model comparison

To verify the accuracy of the model in this paper, two empirical models were chosen to compare with the viscosity data measured from the experiment. The first method was produced by Urbain [36] which was probably the most commonly used method for predicting the slag viscosity. The second method was commonly known as the Watt and Fereday correlation [42].

Comparison of the measured viscosity predicted by Urbain model, Watt and Fereday correlation and the authors' model for different kinds of coals in this study is shown in Fig. 5. On the whole, it can be seen from the Fig. 5, with the decrease of the temperature, the viscosity of the coal slag increased sharply. The increasing trend of viscosity of the authors' model agreed with the experiment data. The Urbain model and the Watt and Fereday correlation expressed poor coincidence with the experiment data. Comparing the results predicted by the three methods, the authors' model in this paper and the Watt and Fereday correlation agreed with the experiment data in the high temperature section. The Urbain model was different with the experiment data in this range. When the temperature was further decreased, the prediction of the Watt and Fereday correlation appeared obvious difference with the experiment data. The Urbain model and the authors' model were in line with the experiment data. T_{cv} of the two classical models also had a certain gap with the experiment data. With the point of 25 Pa.s, the prediction temperatures of the two classical models had a larger difference with the actual temperature. According to the comparison, it can be concluded that the model obtained by authors had advantages in predicting the viscosity of crystalline slag.

4. Conclusion

In the process of slag crystallization, the crystal morphology changed greatly. Most of the crystals showed acicular shape, and the size of the crystals was relatively large. A small part of the crystals had the performance of square. The morphology of the crystals in the slag had a great influence on the slag viscosity. The viscosity of crystalline slag containing a large amount of crystals was difficult to predict. Therefore, to accurately predict the viscosity change during the crystallization process of the molten slag, a new method for predicting the viscosity of the crystalline slag (CSM) was obtained by using the model of the suspension viscosity given in the previous study. The solid phase volume fraction was calculated on the basis of FactSage. The model was verified by ten typical crystalline slags. It was found that the viscosity calculated by the model agreed with the experiment data, and the absolute error was small which proved the model was available for

predicting the viscosity of crystalline slags. However, a little difference between the experiment data and the FactSage calculation results in the fitting of the viscosity at high temperature section was existed. Therefore, the problem of determining the liquid phase viscosity and solid phase volume fraction should be solved in the future work.

Acknowledgments

This study was supported by the National Natural Science Foundation of China (U1402272), the Foundation of Shanghai Science and Technology Committee (14dz1200100), the National Nature Science Foundation of China (21376082), and the Foundation of State Key Laboratory of Coal Conversion (Grant No. J16-17-301).

References

[1] Yamashita K, Barreto L. Energyplexes for the 21st century: coal gasification for co-producing hydrogen, electricity and liquid fuels. Energy 2005;30:2453–73.
[2] Gong X, Lu WX, Guo XL, Dai ZH, Liang QF, Liu HF, et al. Pilot-scale comparison investigation of different entrained-flow gasification technologies and prediction on industrial-scale gasification performance. Fuel 2014;129:37–44.
[3] Krishnamoorthy V, Pisupati S. A critical review of mineral matter related issues during gasification of coal in fixed, fluidized, and entrained flow gasifiers. Energies 2015;8:10430–63.
[4] Yuan HF, Liang QF, Gong X. Crystallization of coal ash slags at high temperatures and effects on the viscosity. Energy Fuels 2012;26:3717–22.
[5] Oh MS, Brooker DD, De Paz EF, Brady JJ, Decker TR. Effect of crystalline phase formation on coal slag viscosity. Fuel Process Technol 1995;44:191–9.
[6] Fredericci C, Zanotto ED, Ziemath EC. Crystallization mechanism and properties of a blast furnace slag glass. J Non-Cryst Solids 2000;273:64–75.
[7] Xuan WW, Whitty KJ, Guan QL, Bi DP, Zhan ZH, Zhang JS. Influence of CaO on crystallization characteristics of synthetic coal slags. Energy Fuels 2014;28:6627–34.
[8] Xuan WW, Whitty KJ, Guan QL, Bi DP, Zhan ZH, Zhang JS. Influence of Fe_2O_3 and atmosphere on crystallization characteristics of synthetic coal slags. Energy Fuels 2015;29:405–12.
[9] Xuan WW, Whitty KJ, Guan QL, Bi DP, Zhan ZH, Zhang JS. Influence of SiO_2/Al_2O_3 on crystallization characteristics of synthetic coal slags. Fuel 2015;144:103–10.
[10] Xuan WW, Zhang JS, Xia DH. Crystallization characteristics of a coal slag and influence of crystals on the sharp increase of viscosity. Fuel 2016;176:102–9.
[11] Shen ZJ, Li RX, Liang QF, Xu JL, Liu HF. Effect of cooling process on the generation and growth of crystals in coal slag. Energy Fuels 2016;30:5167–73.
[12] Louhichi A, Tamborini E, Ghofraniha N, Caton F, Roux D, Oberdisse J, et al. Nucleation and growth of micellar polycrystals under time-dependent volume fraction conditions. Phys Rev E 2013:87.
[13] Karamanov A, Pelino M. Crystallization phenomena in iron-rich glasses. J Non-Cryst Solids 2001;281:139–51.
[14] Păcurariu C, Lazău I. Non-isothermal crystallization kinetics of some glass-ceramics with pyroxene structure. J Non-Cryst Solids 2012;358:3332–7.
[15] Xu J, Zhao F, Guo QH, Yu GS, Liu X, Wang FC. Characterization of the melting behavior of high-temperature and low-temperature ashes. Fuel Process Technol 2015;134:441–8.
[16] Gan L, Zhang CX, Zhou JC, Shangguan FQ. Continuous cooling crystallization kinetics of a molten blast furnace slag. J Non-Cryst Solids 2012;358:20–4.
[17] Shen ZJ, Liang QF, Zhang BB, Xu JL, Liu HF. Effect of continuous cooling on the crystallization process and crystal compositions of iron-rich coal slag. Energy Fuels 2015;29:3640–8.
[18] Trasi NS, Baird JA, Kestur US, Taylor LS. Factors influencing crystal growth rates from undercooled liquids of pharmaceutical compounds. J Phys Chem B 2014;118:9974–82.
[19] Burkhard DJM. Nucleation and growth rates of pyroxene, plagioclase, and Fe-Ti oxides in basalt under atmospheric conditions. Eur J Mineral 2005;17:675–86.
[20] Kondratiev A, Jak E. Predicting coal ash slag flow characteristics (viscosity model for the Al_2O_3–CaO–'FeO'–SiO_2 system). Fuel 2001;80:1989–2000.
[21] Ilyushechkin AY, Hla SS, Roberts DG, Kinaev NN. The effect of solids and phase compositions on viscosity behaviour and T_{CV} of slags from Australian bituminous coals. J Non-Cryst Solids 2011;357:893–902.
[22] Zhang GH, Zhen YL, Chou KC. Influence of TiC on the viscosity of CaO–MgO–Al_2O_3–SiO_2–TiC suspension system. ISIJ Int 2015;55:922–7.
[23] Kong LX, Bai J, Li W, Wen XD, Li XM, Bai ZQ, et al. The internal and external factor on coal ash slag viscosity at high temperatures, Part 1: effect of cooling rate on slag viscosity, measured continuously. Fuel 2015;158:968–75.
[24] Kong LX, Bai J, Li W, Wen XD, Liu XC, Li XM, et al. The internal and external factor on coal ash slag viscosity at high temperatures, Part 2: effect of residual carbon on slag viscosity. Fuel 2015;158:976–82.
[25] Kong LX, Bai J, Li W, Wen XD, Li XM, Bai Z, et al. The internal and external factor on coal ash slag viscosity at high temperatures, Part 3: effect of CaO on the pattern of viscosity–temperature curves of slag. Fuel 2016;179:10–6.
[26] Zhang Gh, Zhen Yl, Chou KC. Viscosity and structure changes of CaO-SiO_2-Al_2O_3-CaF_2 Melts with substituting Al_2O_3 for SiO_2. J Iron Steel Res Int 2016;23:633–7.
[27] Feng C, Chu MS, Tang J, Qin J, Li F, Liu ZG. Effects of MgO and TiO_2 on the viscous behaviors and phase compositions of titanium-bearing slag. Int J Miner Metall Mater 2016;23:868–80.
[28] Wang ZG, Bai J, Kong LX, Wen XD, Li XM, Bai ZQ, et al. Viscosity of coal ash slag containing vanadium and nickel. Fuel Process Technol 2015;136:25–33.
[29] Ilyushechkin AY, Hla SS. Viscosity of high-iron slags from Australian coals. Energy Fuels 2013;27:3736–42.
[30] Folkedahl BC, Schobert HH. Effects of atmosphere on viscosity of selected bituminous and low-rank coal ash slags. Energy Fuels 2005;19:208–15.
[31] Kondratiev A, Jak E. Modeling of viscosities of the partly crystallized slags in the Al_2O_3-CaO-"FeO"-SiO_2 system. Metall Mater Trans B 2001;32:1027–32.
[32] Hosseini M, Ghader S. A model for temperature and particle volume fraction effect on nanofluid viscosity. J Mol Liq 2010;153:139–45.
[33] Ramacciotti M, Journeau C, Sudreau F, Cognet G. Viscosity models for corium melts. Nucl Eng Des 2001;204:377–89.
[34] Browning GJ, Bryant GW, Hurst HJ, Lucas JA, Wall TF. An empirical method for the prediction of coal ash slag viscosity. Energy Fuels 2003;17:731–7.
[35] Fulcher GS. Analysis of recent measurements of the viscosity of glasses. J Am Ceram Soc 1925;8:339–55.
[36] Urbain G. Viscosity of silicate melts. Trans J BrCeram Soc 1981;80:139.
[37] Weymann HD. On the hole theory of viscosity, compressibility, and expansivity of liquids. Colloid Polym Sci 1962;181:131–7.
[38] Kalmanovitch DP, Frank M. An effective model of viscosity for ash deposition phenomena. Miner Matter Ash Deposition Coal 1988:89–101.
[39] Kondratiev A, Jak E. Review of experimental data and modeling of the viscosities of fully liquid slags in the Al_2O_3-CaO-'FeO'-SiO_2 system. Metall Mater Trans B 2001;32:1015–25.
[40] Hurst H, Novak F, Patterson J. Viscosity measurements and empirical predictions for fluxed Australian bituminous coal ashes. Fuel 1999;78:1831–40.
[41] Reid WT. External Corrosion and Deposits: Boilers and Gas Turbines. American Elsevier Publishing; 1971.
[42] Watt JD, Fereday F. Flow properties of slags formed from ashes of british coals. 1. Viscosity of homogeneous liquid slags in relation to slag composition. Journal of the Institute of. Fuel 1969;42:99.